Chapter 5

Analysis of independent components in biomedical signals

Ricardo Vigário, Jaakko Särelä, Elina Karp, Jarkko Ylipaavalniemi

5.1 Biomedical data analysis

Ricardo Vigário, Jaakko Särelä, Elina Karp, Jarkko Ylipaavalniemi

In the period spanned by this report, we have enlarged our ongoing collaboration with the Brain Research Unit of the Helsinki University of Technology to the recently established Advanced Magnetic Imaging Centre, from the same university. We further explored contacts with the radiology department of Helsinki University Central Hospital. International collaborations were as well pursued with very positive outcomes.

The global list of publications, at the end of this report, contains further references to this work. The ones in this section should give a good starting point to the understanding of the results achieved within the project.

Coherence studies

Strong coherence around 20 Hz is known to exist between the MEG recording the primary motor cortex and the contralateral electromyogram (EMG) during isometric muscle contraction. In [2, 1], we applied a temporal decorrelation technique to identify the underlying brain areas producing signals coherent with the EMG. The algorithm chosen, the temporal decorrelation source separation (TDSEP [3]), exploits efficiently the temporal structure present in the data.

To reduce the occurrence of overlearning of the TDSEP algorithm in such high-dimensional data set (204 channels were recorded), a suitable reduction was performed during its whitening stage. Yet, we are now not necessarily interested in reconstructing the original data, but rather in the preservation of the corticomuscle coherence between the components and the reference EMG. Hence, we choose to sort the principal components according to their coherence power, discarding those that contribute the least to the coherence, in the vicinity of the characteristic 20 Hz.

Figure 5.1 presents the top 7 coherences between the 204 MEG channels and the right-hand EMG. The strongest coherence peaks around 14 Hz, which is close to the values suggested in the literature.

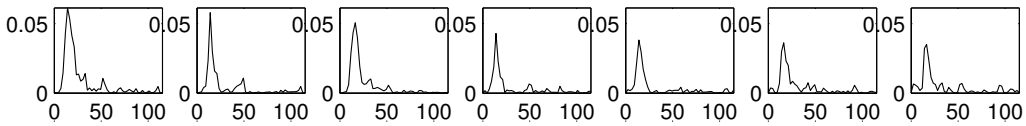

Figure 5.1: Strongest coherences between the MEG channels and the left-hand EMG.

In Fig. 5.2, the 7 most coherent TDSEP components are shown. Only the first signal shows significant coherence values (even higher than that of any single MEG channel). The

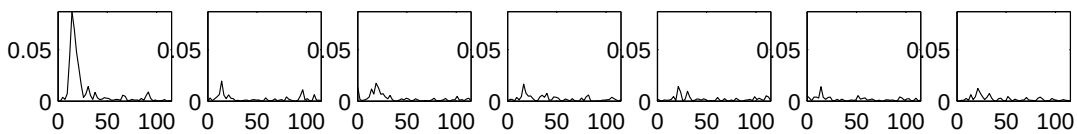

Figure 5.2: Coherence plots for the 7 most coherent TDSEP components.

field patterns associated with several TDSEP components, see Fig. 5.3, show selectivity over the central left and right hemispheres, and are well modeled by current dipoles in the respective primary motor cortices.

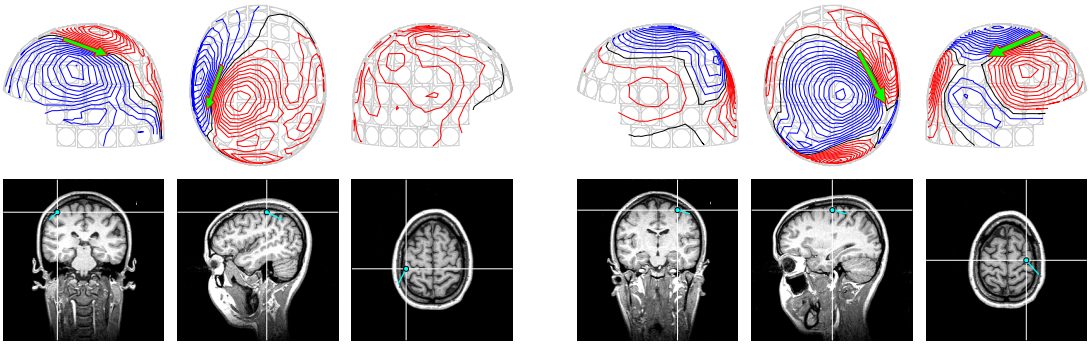

(a) (b)

Figure 5.3: Field patterns and equivalent current dipoles for the 1st TDSEP component (a) and the 25th (b).

References

[1] Ricardo Vigário and Ole Jensen. Identifying cortical sources of corticomuscle coherence during bimanual muscle contraction by temporal decorrelation. In *Proc. of the 7th Int. Symp. on Signal Proc. and its Applications (ISSPA'03)*, pages 109 – 112, Paris, 2003.

[2] Ricardo Vigário, Ole Jensen, and Riitta Hari. Identifying cortical sources of corticomuscle coherence during bimanual muslce contraction by ICA. In *Proc. of the 13th Int. Conf. on Biomagnetism (BIOMAG'02)*, page 1005, Jena, Germany, 2002.

[3] Andreas Ziehe and Klaus-Robert Müller. TDSEP – an effective algrithm for blind separation using time structure. In *Proc. Int. Conf. on Artificial Neural Networks (ICANN'98)*, pages 675 – 680, Skövde, Sweden, 1998.

Structural MRI

Magnetic resonance imaging (MRI) is a non-invasive technique capable of producing 3D high resolution images of the human body. It relies on the interaction between the intrinsic magnetic fields of nuclei and strong externally applied magnetic fields and radiofrequency pulses. By adjusting internal parameters, related to the onset of the external pulses and fields, one can change the focus of the image on different anatomical and physiological properties of the tissues. A realistic simulation of those differences is depicted in Fig. 5.4a [1], for the standard T1, T2 and PD (proton density) parameter set. From the

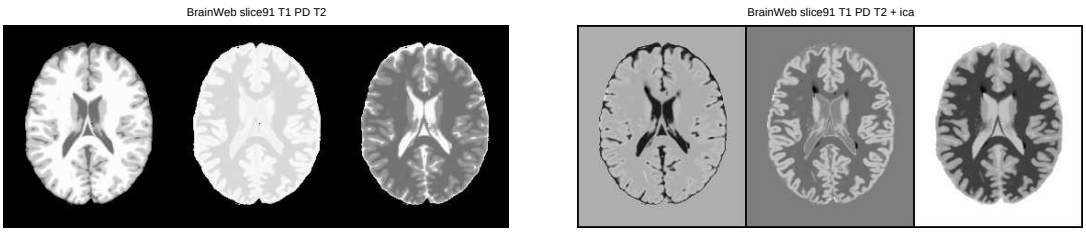

(a) (b)

Figure 5.4: Simulated MRI slices for different imaging parameters (a) and the independent components (b).

observation that different tissues react differently to the changes of parameters, together with an approximation that each image is composed of linear mixtures of independent tissues, we have used ICA as a mean to isolate each such tissue. This was performed with both simulated and real MRI scans, for various MRI parameter sets. These included the standard 3, to a much enlarged 13 set. The result of applying ICA to the 3 image simulated data can be seen in Fig. 5.4b.

A quick glance to Fig. 5.4b reveals that the independent components show greater tissue selectivity than the original images. The first frame, e.g., depicts nearly only cerebrospinal fluid, whereas the second frame show clearly multiple sclerosis (black spots), invisible in the classification of the raw data.

Tissue segmentation was as well studied on both unprocessed and ICA-processed data, by clustering and judiciously coloring Self-Organizing Maps (SOMs), trained for each data set. The results, for the same simulated data, are shown in Fig. 5.5.

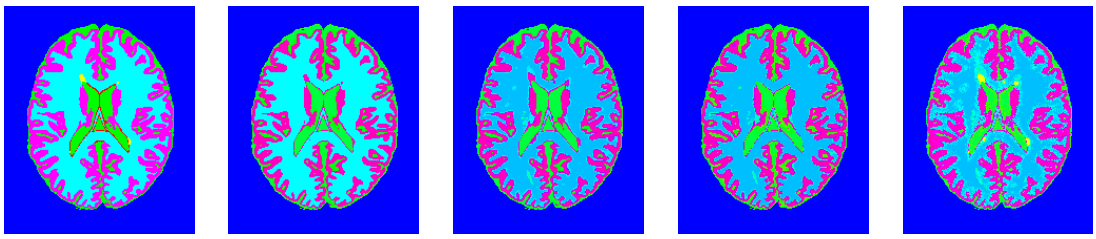

(a) (b) (c) (d) (e)

Figure 5.5: Ground truth segmentation for the simulated MRI data (a), and that found in SOM for the 3-image (b) and the 13-image (c) data sets. Same for ICA-preprocessed in (d) and (e).

Most structures are already segmented in the unprocessed data. Yet, the multiple sclerosis is somewhat hard to detect there, and is only clearly visible from the ICA processed

13-image data set. This suggests that both the increase of multispectral MRI and the pre-processing are efficient strategies for isolating such tissues.

Similar results were observed for real data [1]. Additionally, the application of ICA to the innovation portion of the MR image yields somewhat better results than the ones observed for the normal use of ICA.

ICA preprocessing of MRI data was successfully used in a different segmentation approach, where the acting principle is now a semi-unsupervised use of Support Vector Machines [2]. The results are very promising (see Fig. 5.6).

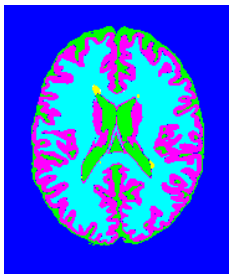

Figure 5.6: Segmentation of the simulated data using support vector machines.

Functional MRI

Functional magnetic resonance imaging (fMRI) is based on similar principles as structural MRI. Yet, with the cost of a clear decrease in spatial resolution, the collection of a full volume in fMRI takes much less time, allowing for multiple images in succession.

Different oxygenation levels in the blood result in variations of its magnetic properties, hence in the MR image. Using this principle, together with a clear pattern of stimulation, several images are collected. One such pattern is the recording of n images with stimulus, followed by a series of m in resting mode. Standard analysis then look for voxels, or combinations of voxels, which show an activation pattern in relation to the stimulus. When ICA is used to process fMRI data, no such stimulus-lock is imposed.

The linear model assumed in our fMRI study is 'transposed' to the one used in EEG and MEG recordings, i.e., the independence is not assumed to exist in time, but rather in space. The mixing matrix, which gives the spatial patterns of activation in EEG and MEG is now the temporal course of the spatially independent components.

Fig. 5.7 shows that, even in a blind source separation framework, ICA is capable of identifying components in clear agreement with the particular auditory type of stimulation. This preliminary study [3] showed as well that brain activity, as well as artifacts, with no relation to the temporal activation of the stimulus can be detected. Due to the lack of relation to the stimulus, those signals would be very hard to identify using classical processing.

Furthermore, even though one asset of ICA is to be unlocked to the stimulus, one may find useful to search for methods that incorporate additional (small) amounts of prior information. These can be based on, *e.g.*, semi-blind source separation 2 or Bayesian methods 3

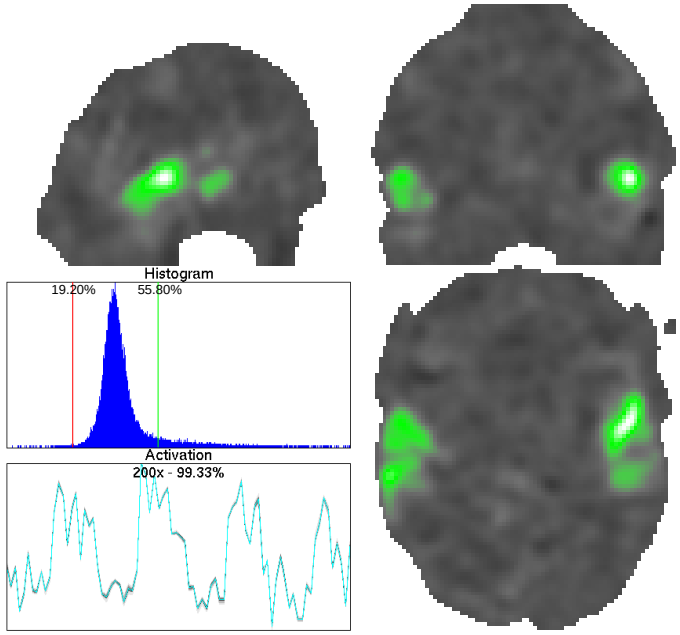

Figure 5.7: Independent component, directly related to the auditory stimulus.

References

[1] Elina Karp, Hugo Gävert, Jaakko Särelä, and Ricardo Vigário. Independent component analysis decomposition of structural MRI. In *Proc. of the 2nd IAESTED Int. Conf. on Biomed. Eng. (BioMED'04)*, Innsbruck, Austria, 2003.

[2] Elina Karp and Ricardo Vigário. Unsupervised MRI tissue classification by support vector machines. In *Proc. of the 2nd IAESTED Int. Conf. on Biomed. Eng. (BioMED'04)*, Innsbruck, Austria, 2003.

[3] Jarkko Ylipaavalniemi and Ricardo Vigário. ICA decomposition of an auditory functional MRI reveals thalamic activation. Submitted to a conference.